A CRN SIMULATION FOR EMISSION POLLUTANTS PREDICTION IN LEAN PREMIXED GAS TURBINE COMBUSTOR

Nguyen Thanh Hao[1], Nguyen Thanh Nam[1], and Jungkyu Park[2]

[1] Dcselab, Ho Chi Minh University of Technology, Ho Chi Minh City, Vietnam, Tel: 84-8-919034504,
e-mail: nguyenthanhhao@hui.edu.vn
[2]Department of Mechanical Engineering, Konkuk University, Seoul, Korea, Tel: 82-1091634628,
e-mail: jungkyu@konkuk.ac.kr

Abstract

This study presents the use of a new CRN (Chemical Reactor Network) model and non-uniform injectors to predict the emission pollutant in the lean premixed gas turbine combustor. The CRN uses the information from the CFD (Computational Fluid Dynamics) combustion analysis with two injectors of CH_4-air mixture. The experiment and the modeling focus on the output of the turbine combustor and the optimized fuel load. The injectors of CH_4-air mixture have different lean equivalence ratio, and they control the fuel flow to stabilize the combustion and adjust the combustor's equivalence ratio. The non-uniform injector is applied to improve the burning process of the turbine combustor. The results of the new CRN emission predictions for the gas turbine combustor show very good agreement with the experimental data from Korea Electric Power Research Institute. The new CRN model is a valuable tool in the evaluation of the pollution formation and the performance of the turbine combustor systems.

Introduction

Control of pollutant emissions is a major factor in the design of modern combustion systems. The major pollutants produced in the combustion process are nitrogen oxides (NO and NO_2), carbon monoxide (CO) and sulphur oxides (SO_2 and SO_3). Nitrogen oxides (also called NOx) are one of the most toxic pollutants in the atmosphere and are well known as a destroyer of the stratospheric ozone and a precursor of the acid rain. In addition, the fuel price is high and the combustion efficiency is low, which are also greater emphasis.

Simplified CRN models for NOx production rates in the lean-premixed combustion is proposed by Nicol, D. G., Malte, P. C., and Steele, R. C. [1-2]. NOx formation in the lean premixed combustion of CH_4 in a high-pressure jet-stirred reactor is introduced by Bengtson, K. U. M., et al. [3]. Variables effecting NOx formation in the lean-premixed combustion is proposed by Steel, R.C. [4-5]. The combustion of fuels that contains no nitrogen, but NOx is formed by three chemical mechanisms or routes that involve nitrogen from the air: Zeldovich mechanism, Fenimore mechanism, and N_2O-intermediate mechanism. The chemical reactor network model is constructed to be a valuable tool in the evaluation of the pollution formation. The simple two- or three-idealized reactor scheme has been found useful in the modeling researched by Rutar, T. and Malte, P.C. [6]. The development of a four-idealized reactor scheme CH_4 oxidation-NO formation mechanism for the lean premixed gas turbine combustion was introduced by Nicol, D. G., et al. [7]. The CRN development based on the CFD solution of the combustor using eight-idealized reactor scheme was introduced by Novosselov [8].

In this study, based on the actual geometry of the turbine combustor DGT5 and depending on the load which was predicted, the new chemical reactor network model is constructed to predict NOx and CO emission pollutants in the lean premixed turbine combustor.

This research is somewhat different from the previous ones, being more descriptive and less theoretical. The CFD modeling has ability to provide the valuable insight on the flow and the temperature fields of the combustor, which are difficult to obtain from the experiment. While CFD is a valuable tool to predict the flow and the temperature fields, this method cannot incorporate the complicated chemistry of the detailed chemical kinetic mechanisms. CFD cannot always accurately predict the emission pollutants; therefore, a hybrid CFD-CRN model is used to predict NOx and CO in the mixer CH4-air combustion. NOx and CO will be predicted by using the CRN model which is constructed from the information obtained by CFD. The CRN development was based on the CFD solution of the turbine combustor using twenty-four-idealized reactor scheme.

CRN Combustion Modeling

CFD Analysis

The CFD-predicted flow patterns include the flame shape and the location, the entrance of the dome air and gas from the main recirculation zone into the flame. These flow patterns are treated by adjusting the flow splits between the corresponding elements of the network. The analysis includes a three-step EBU model which was performed by using a simple interpretation of the results of the flame. Temperature was used to separate the flame zone which was replaced by simple reactors.

The system modeled consists of a combustor liner, an injector completed with the main circuit, and a pilot circuit. The major design and the operating parameters of the modeled combustor are similar to those of typical industrial gas turbine combustor. The mean axial velocity profiles of the injector are determined based on the profiles of the swirl ratio and the non-uniform swirl mixture injector. The CRN model is configured from the entrance, considering the mixture of fuel and air and the occurrence of the back-flash phenomenon, because CH4-air separated analysis is applied to the entrance of the gas turbine combustor.

Star-CCM offers a wide variety of turbulence modeling capabilities. These may be subdivided into four categories: Eddy viscosity models (k-ε, k-ω, k-ε-f$_\mu$, k-ε-v^2-f…), Reynolds stress models (RSM), Large eddy simulation models (LES), Detached eddy simulation models (DES). In this research, the flow involves a turbulent, compressible and multi-component gas whose components are reacting chemically. Therefore, the k-ε turbulence model is used for the wall insulation combustion chamber conditions. In Star-CCM, however, these effects are modeled as in the standard k-ε model. The turbulent kinetic energy and turbulence dissipation rate are determined by solving their modeled transport equations (1) ÷ (2). CFD computation, with an appropriate turbulence model, has ability to provide valuable insight on the flow and temperature fields of the combustor, which are difficult to obtain experimentally.

$$\frac{\partial}{\partial t}(\rho k) + \frac{\partial}{\partial x_j}\left[\rho u_j k - \left(\mu + \frac{\mu_t}{\sigma_k}\right)\frac{\partial k}{\partial x_j}\right] = \mu_t(P + P_B) - \rho\varepsilon - \frac{2}{3}\left(\mu_t\frac{\partial u_j}{\partial x_j} + \rho k\right)\frac{\partial u_i}{\partial x_i} + \mu_t P_{NL} \quad (1)$$

$$\frac{\partial}{\partial t}(\rho\varepsilon) + \frac{\partial}{\partial x_j}\left[\rho u_j\varepsilon - \left(\mu + \frac{\mu_t}{\sigma_\varepsilon}\right)\frac{\partial\varepsilon}{\partial x_j}\right] = C_{\varepsilon1}\frac{\varepsilon}{k}\left[\mu_t P - \frac{2}{3}\left(\mu_t\frac{\partial u_i}{\partial x_i} + \rho k\right)\frac{\partial u_i}{\partial x_i}\right] + C_{\varepsilon1}\frac{\varepsilon}{k}\mu_t P_{NL}$$
$$-C_{\varepsilon2}\rho\frac{\varepsilon^2}{k} + C_{\varepsilon3}\frac{\varepsilon}{k}\mu_t P_B + C_{\varepsilon4}\rho\varepsilon\frac{\partial u_i}{\partial x_i} \tag{2}$$

where

$$P = S_{ij} \frac{\partial u_i}{\partial x_j} \tag{3}$$

$$P_B = -\frac{g_i}{\sigma_{h,t}} \frac{1}{\rho} \frac{\partial \rho}{\partial x_i} \tag{4}$$

$$P_{NL} = -\frac{\rho}{\mu_t} \overline{u_i' u_j'} \frac{\partial u_i}{\partial x_j} - \left[P - \frac{2}{3} \left(\frac{\partial u_i}{\partial x_i} + \frac{\rho k}{\mu_t} \right) \frac{\partial u_i}{\partial x_i} \right] \tag{5}$$

C_μ is the isotropic turbulent viscosity and given by the Prandtl-Kolmogorov relation

$$\mu_t = C_\mu \rho \frac{k^2}{\varepsilon} \tag{6}$$

The model constants are assigned the following standard values: $C_\mu = 0.09$, $C_{\varepsilon 1} = 1.44$, $C_{\varepsilon 2} = 1.92$, $C_{\varepsilon 3} = 1.44$ for $P_B > 0$ or $C_{\varepsilon 3} = 0$ for other, $C_{\varepsilon 4}- = 0.33\sigma$,$_k = 1.0$ and $_\varepsilon \sigma = 1.22$. The air inlet velocity and the fuel inlet velocity of the different load (1.0N, 0.8N, 0.6N, idle) are based on the experimental conditions (Table 1). In the properties of Star-CCM window, these standard values are entered into each node for setting model parameters.

The simulation performed in the model of CH_4-air combustion is repeated using a three-step reaction of the following forms

$$CH_4 + 0.5O_2 \rightarrow CO + 2H_2 \tag{7}$$

$$CO + 0.5O_2 \rightarrow CO_2 \tag{8}$$

$$H_2 + 0.5O_2 \rightarrow H_2O \tag{9}$$

The Reactions (7) ÷ (9) themselves are defined by specifying the amounts (in kilomoles) of the participating leading reactants, reactants and products. In the properties of Star-CCM window, these amounts are entered into each node for the stoichiometry coefficient.

The combustion model is used to calculate the reaction state space, the concentrations of the various species present in a chemical reaction, density, viscosity, and temperature. In this study, a CH_4 combustion case is set up using the Presumed Probability Density Function (PPDF) reaction model for premixed flames. The model assumes adiabatic conditions and a local instantaneous chemical equilibrium. In the PPDF model, a few parametric variables such as the mean mixture fraction are tracked on the grid. The mean species concentrations, temperature and density are obtained as functions of mean parametric variables, after an averaging process around a presumed probability distribution that is considered to represent turbulent fluctuations. Under this assumption, if one defines a mixture fraction

$$f = \frac{m_m}{m_m + m_p} \tag{10}$$

where m_m is the total mass of all atoms originating from the main inlet at any spatial location, and m_p is the total mass of all atoms originating from the pilot inlet, it can be seen that f is a converted scalar. The equation for such a scalar is simple; f is transported by convection and diffusion, and can accumulate locally, but there is no f production. Therefore:

$$\frac{\partial}{\partial t}(\rho f) + \nabla \bullet [\rho U f - \rho D_f \nabla f] = 0 \tag{11}$$
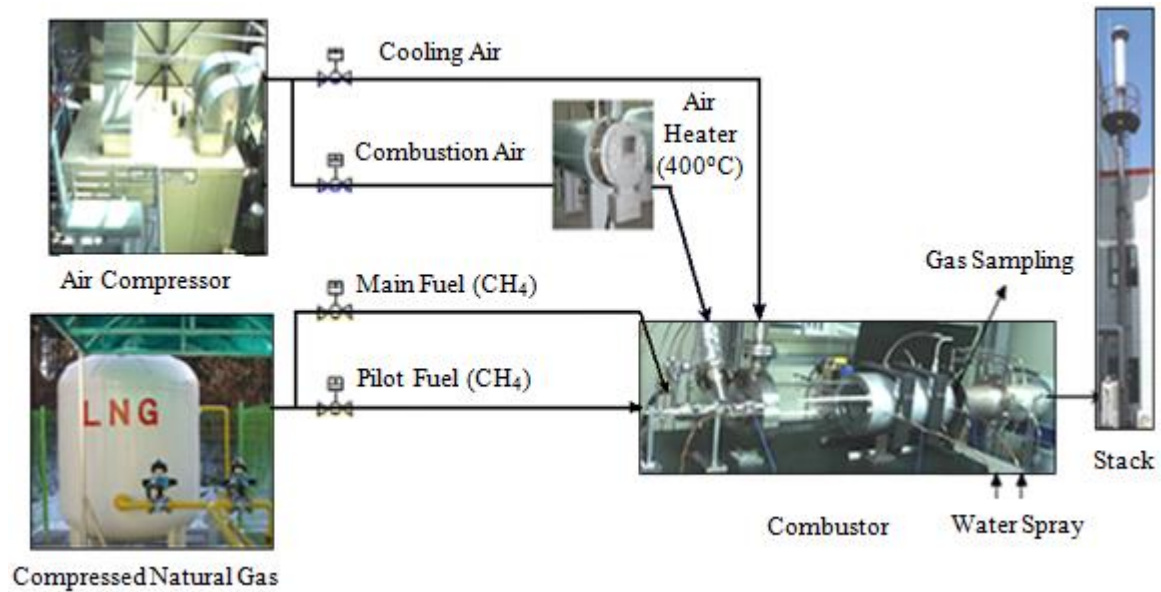
Figure 1. The experiment schematic measurement

The overall structure of the gas turbine combustor system (Figure 1) includes an air compressor, an air heater, a compressed natural gas, a combustor, two gas turbine burners, and an exhaust processing unit. The control instrumentation consists of the ICCD camera and the image processing controller, etc.

The experiment parameters are based on combustion conditions. The external temperature is 298K, after passing through compressor, the temperature is 650K. The pressure and the other combustion parameters are based on the maximum load (1.0N load) and the minimum load (idle load).

In order to understand the effect of the injector CH_4-air mixing profile on the flame position and the emission levels, this study will calculate the profile of the non-uniform injector. The mixture of fuel and air in both main injector and pilot injector are not the same. At the idle load, the overall equivalent ratio of the pilot injector is less than 0.7, and the lower overall equivalent ratio is 0.166. The overall equivalent ratio of the main injector and the pilot injector at 1.0N load is 0.422, at 0.8N load is 0.367, and at 0.6N load is 0.314. More detailed conditions are shown in Table 1.

The combustion chamber boundary is a cylindrical shape using the grid to reduce the computational time as shown in Figure 2. A two-dimensional grid consisting of 190,000 cells is used. The modeling assumptions used in the numerical simulation are listed in Table 2. In order to adequately resolve the gradients that exist in the flame, the grid resolution is refined in the pilot flame region and the boundary layer effect.

Table 1. Experimental Conditions for Combustor

Description	Unit	Normal condition ($T_{air}= 15^0C$)			
		1.0N	**0.8N**	**0.6N**	**Idle**
Air flow rate into the flame tubes	kg/s	0.08697	0.08912	0.09144	0.09842
Combustion Air	Nm^3/hr	266.93	275.56	284.83	317.37
Total pressure of air after the compressor	Mpa	0.1	0.1	0.1	0.1
Total hourly fuel consumption	Slpm	174.85	155.76	136.62	77.89
Fuel consumption of the 1st fuel channel (pilot)	Slpm	68.8	77.88	82.5	77.89
Fuel consumption of the 2nd fuel channel (main)	Slpm	106.05	77.88	54.12	0
Overall equivalence ratio	-	0.422	0.367	0.314	0.166

Table 2. Modeling Assumptions and Boundary Conditions for Combustor

Numerical domain	Polyhedral 190,000 cells
Solver	Reynolds Averaged Navier-Stokes
Turbulence model	High Reynolds k-ε model
Wall condition	Cyclic wall-30^0 adiabatic
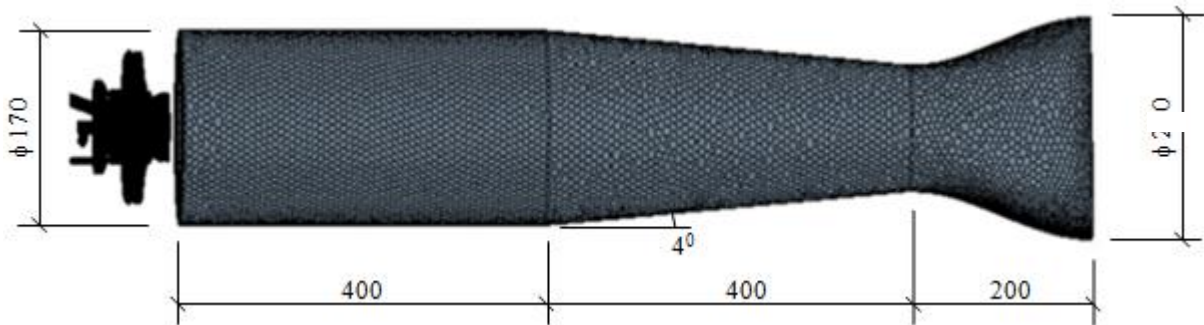
Figure 2. Computation grid for CFD modeling of gas turbine combustor

The combustor used in this study has the same shape and size of the gas turbine combustor DGT-5 as shown in Figure 2. The experimental simulation of a simplified practical and reliable combustor in order to pursue the practical and physical changes are at the same shape and size, but we need to visualize the liner portions omitted except the cooling air and the dilution air. All parts were fabricated by the same simulation.

The results of the mass fraction of the gas turbine combustor at the entrance with the overall equivalent ratio of 0.7 are shown in Figure 3. The formation of the NOx and CO emissions in the combustor is determined by the post-processing CFD solutions of the flow field. Figure 3 shows the CFD predicted flow patterns and the CRN flow splits of the flame. In the CFD modeling of the modeled combustor (section A-A), it has been found that a very small amount of gas from the main flame enters the dome recirculation zone. Thus,

one percent (1%) of the main flame gas has been assigned to be recycled into the dome recirculation zone. This percentage can change when a different combustor setup is used. In the CFD modeling of the modeled combustor (section B-B), it has been found that ten percent (10%) of the main pilot flame gas has been assigned to be recycled into the main flame, ten percent (10%) of the main pilot flame gas has been assigned to be recycled into the pilot recirculation zone. The fuel-air ratio of the pilot injector is assumed to be in uniform, there is no radial or circumferential variability in the fuel-air mixture. The main pilot stream mixes with gas from the main recirculation zone and the pilot recirculation zone. The post flame zone needs to be split into two streams based on the CFD temperature and the fuel-air equivalence ratio in the center post flame zone and the main post flame zone. In the CFD modeling of the modeled combustor, it has been found that thirty percent (30%) of the post flame gas has been assigned to be recycled into the main pilot. The typical backside cooled gas turbine combustor also has a dilution zone, where dilution air is introduced into the post flame zone to reduce the gas temperature prior to entering the turbine. The simple CRN does not have any secondary dilution addition, so the last PFR element could be used for this purpose.
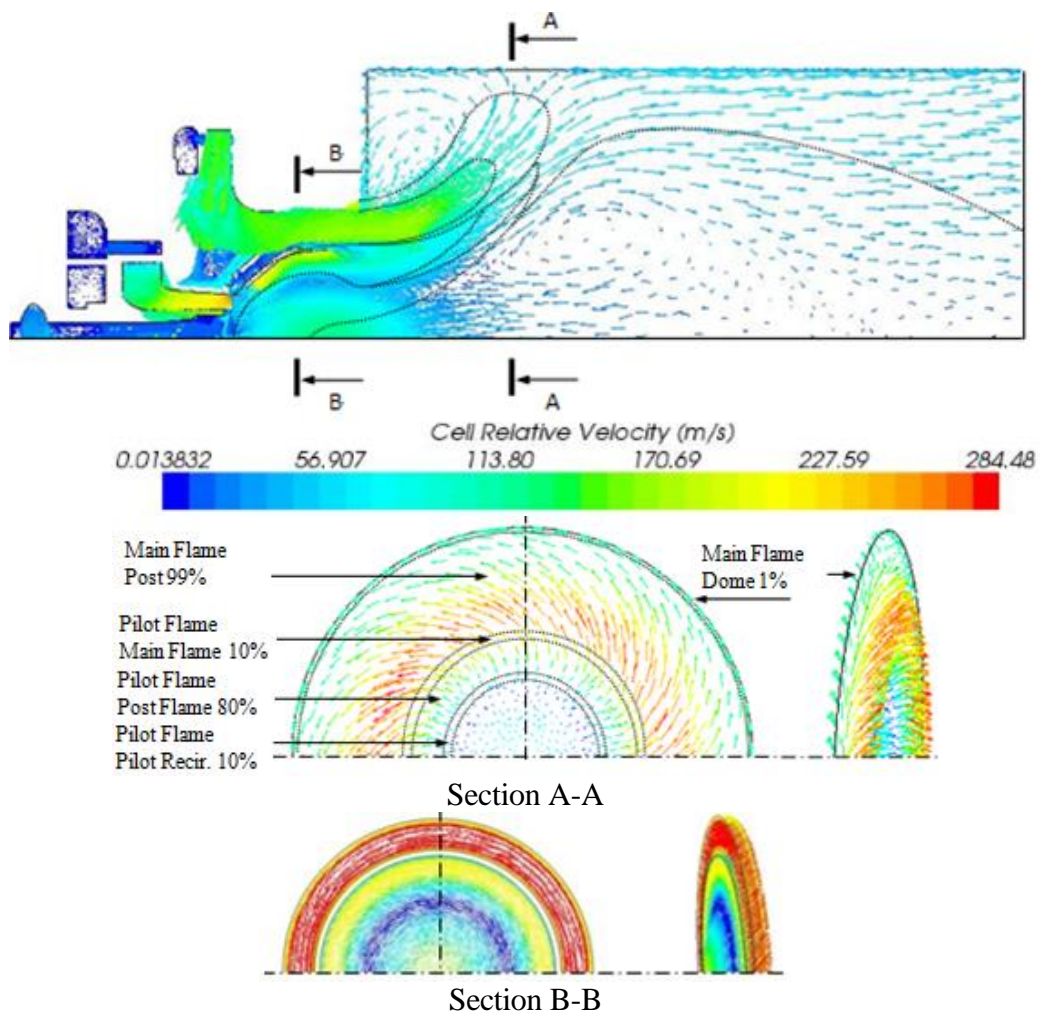
Figure 3. Velocity and mass fraction at the injector outlets
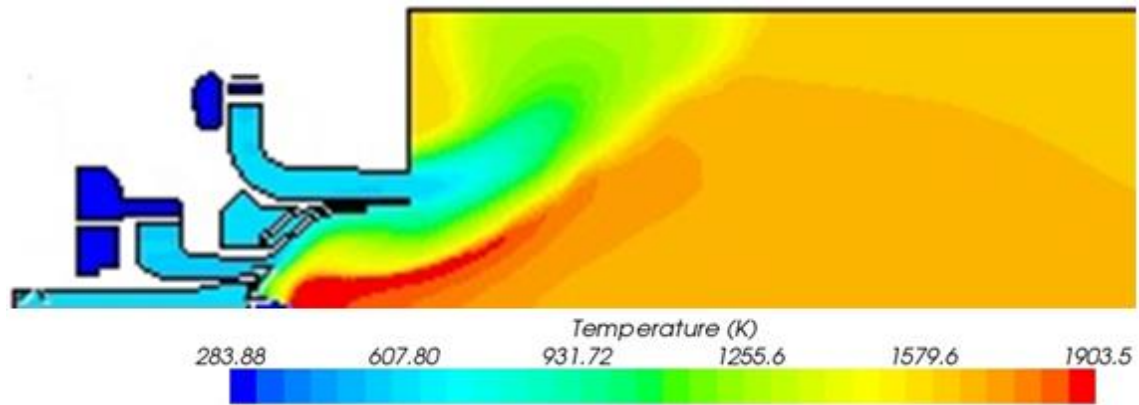
(a) Flame Temperature Surface
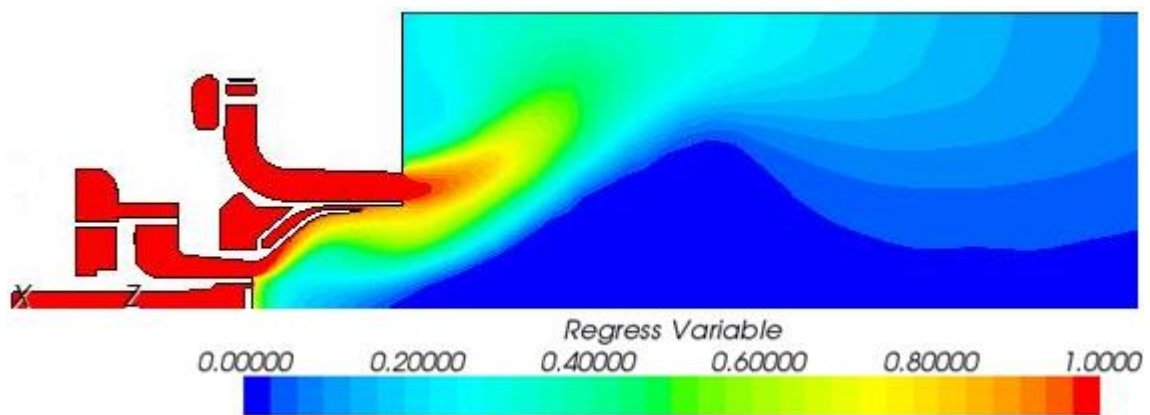
(b) R<u>atio</u> of unburned fuel in a premixed flame
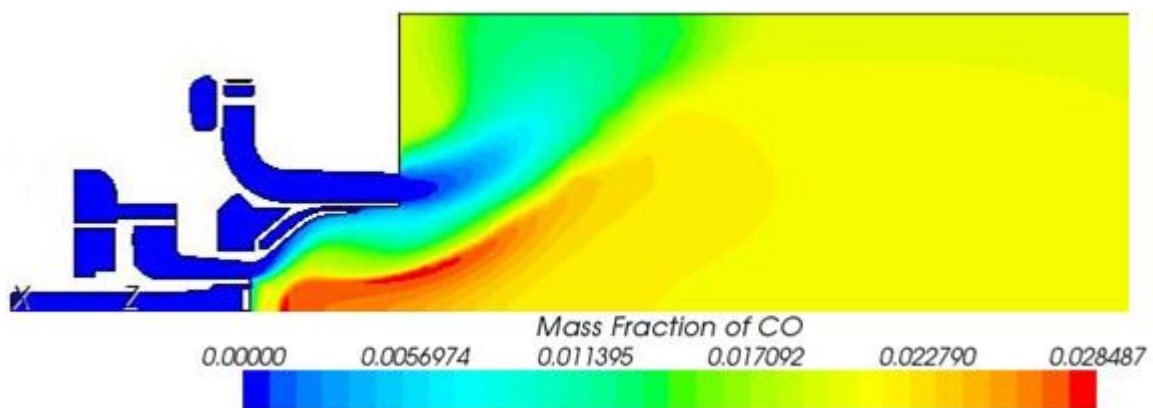
(c) Mass Fraction of CO Surface

Figure 4. Temperature, regress variable and mass fraction contours plot from Star-CCM software showing the presence of the different combustion zones

Temperature, regress variable and mass fraction contours plotted from the 2D CFD simulation show the different combustion zones (Figure 4). A regress variable represents the ratio of fuel that is unburned in a premixed flames, it has a value of 1.0 for an unburned gas mixture and a value of 0.0 for a fully burned mixture.

The different combustion zones in Figure 5 includes the main flame zone, the main recirculation zone, the pilot inner zone, the pilot out post, the pilot median zone and the pilot

recirculation zone. The highest temperature of the flame in the combustion chamber appears on the wall. In the non-uniform mass fraction inlet case, the temperature is up to 1903.5K. The development chemical reactor network modeling of the gas turbine combustor is constructed based on the CFD-predicted flow patterns such as the flame temperature and the volumetric zones (Figure 5), and the entrainment of the dome air and gas from the main recirculation zone into the flame as show in Figure 3.
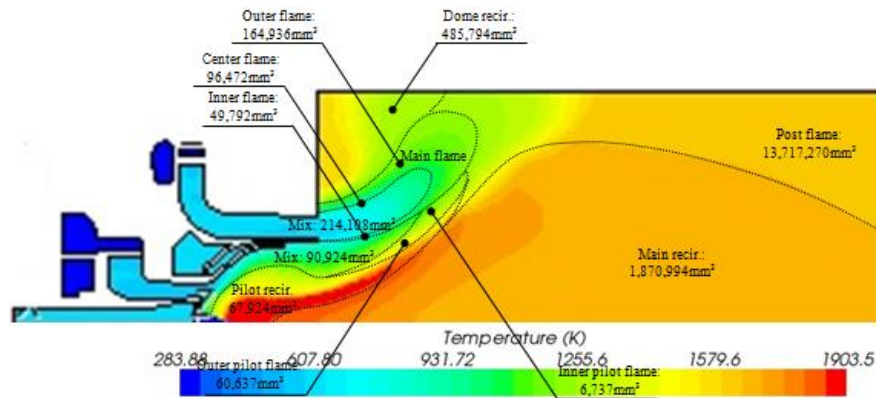
Figure 5. Flame zone mapping onto the CRN

CRN Model Configuration

CRN model is constructed in this study based on Figures 4 and 5. First of all, the recirculation zone consists of PSR which was a fully mixed assumption. According to the results of Figure 5, the temperature of the flame was broken. Subdivision of the flame cross-section of the entrance in order to determine the flow information is used based on the results of Figure 3.

At the idle state, the overall equivalent ratio distribution is up to 0.9. More than 0.05 units from the overall equivalent ratio of 0.7 are divided into two entrances. The overall equivalent ratio ranges from 0.6 to 0.7. One of areas is subdivided into the entrance, so the total entrances are two. The number of the flame zones is also divided into eight zones. The regions of the overall equivalent ratio of 0.7 or more are accounted approximately 20% of the total.

At the 0.6N load, 0.8N load, and 1.0N load state, when the overall equivalent ratio distribution is 0.85, the equivalent ratio does not exist, and the flame zone is divided into eight zones. The regions of the overall equivalent ratio of 0.7 of 0.6N load are accounted approximately 12%. The 1.0N load is accounted approximately 9% of the total.

The CRN model is separated because a non-equivalent portion of the pilot flame was broken. The area consists of more than the overall equivalent ratio of 0.8 is the pilot out 2 to simulate the flame on the wall. The area consists of more than the overall equivalent ratio of 0.7 is the pilot out 1 to simulate the flame inside of the wall. The overall equivalent ratio less than 0.6 are accounted approximately a medium flame. The schematic layout of the 24-element CRN is constructed in this study which based on the CFD-predicted results as shown in Figure 6(a) and it is used to evaluate the CO and NOx emissions based on CHEMKIN software as shown in Figure 6(b).

PSR stands for a perfectly stirred reactor in which mixing to the molecular scale is assumed to happen instantaneously compared to the chemical reaction. The combustion occurs homogeneously in the reactor. PFR stands for a plug flow reactor in which the flow is assumed to move as a plug, and the chemical reaction which proceeds one-dimensionally,

longitudinally mixing in the reactor is assumed to be zero. MIX stands for an element in which the entering streams are uniformly mixed without chemical reaction. The first element in the CRN arrangement is the MIX, which represents the cone shape zone of the inlet mixture where the mixture is not ignited yet. The flame zone, the dome and the main recirculation zone, and the immediate post flame zone are modeled by using PSR, while the post flame zones are modeled by using PFR.

The CRN elements are grouped according to the zones as shown in Figure 6. The main flame zone (MFZ) consists of the main flame, the immediate post flame, and the post flame. The pilot flame zone consists of some of the pilot out, provided by the injector pilot, the pilot media, the pilot recirculation, and the pilot post. The dome recirculation zone (DRZ) consists of the combustor dome air input stream. The center recirculation zone (CRZ) consists of the back-mixed hot product gas flow. The post flame zone (PFZ) consists of the CO burn out zones, as depicted in Figure 5.
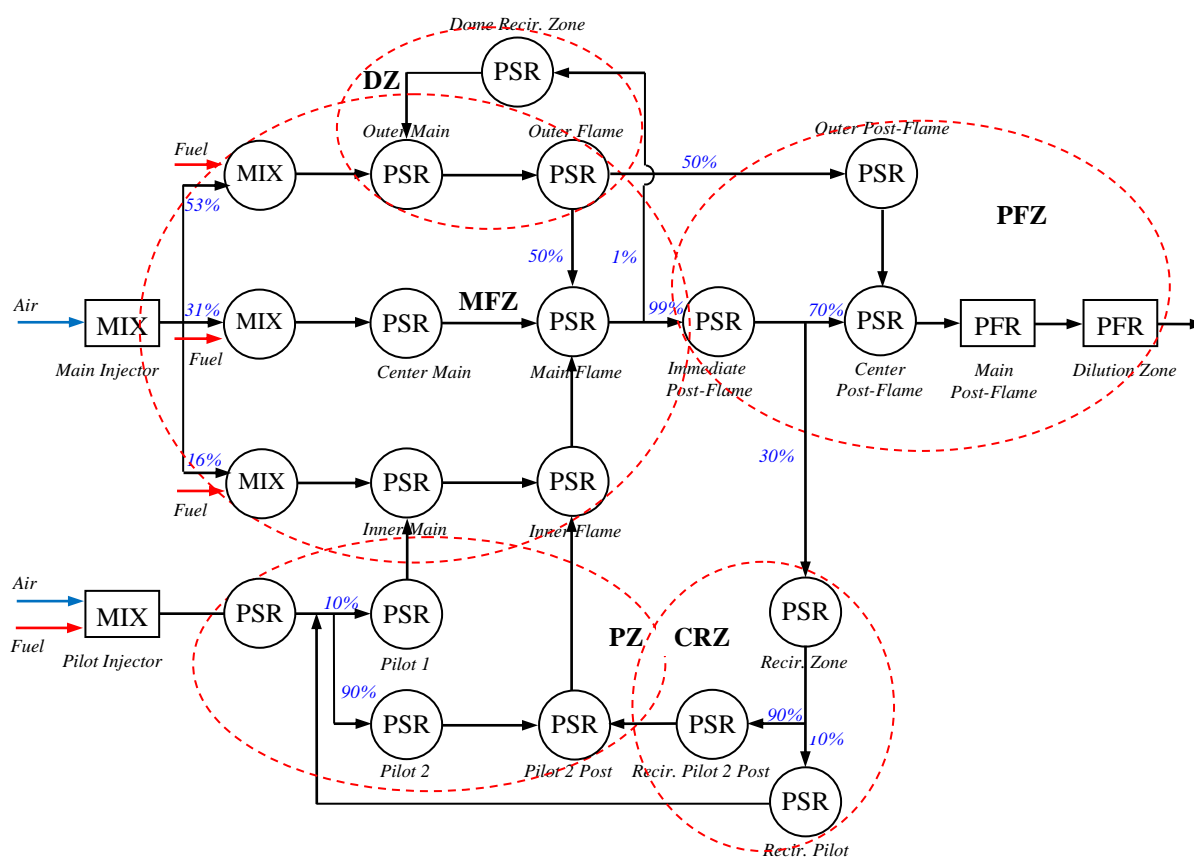
(a) The Schematic Layout of 24-Element CRN
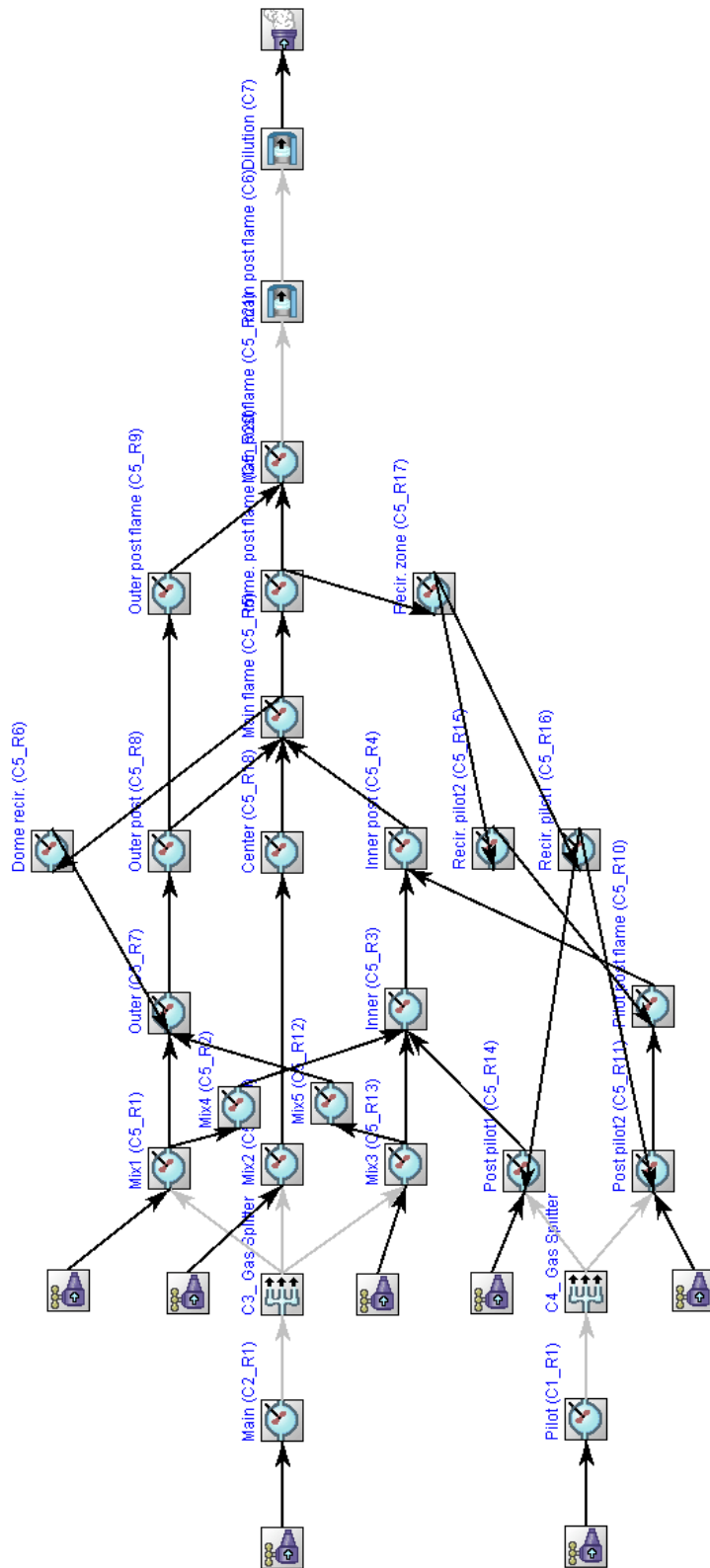
(b) 24-Element CRN for Evaluating the CO and NOx Emissions Based on CHEMKIN Software

Figure 6. 24-Element chemical reactor network of gas turbine combustor

Results and Discussions
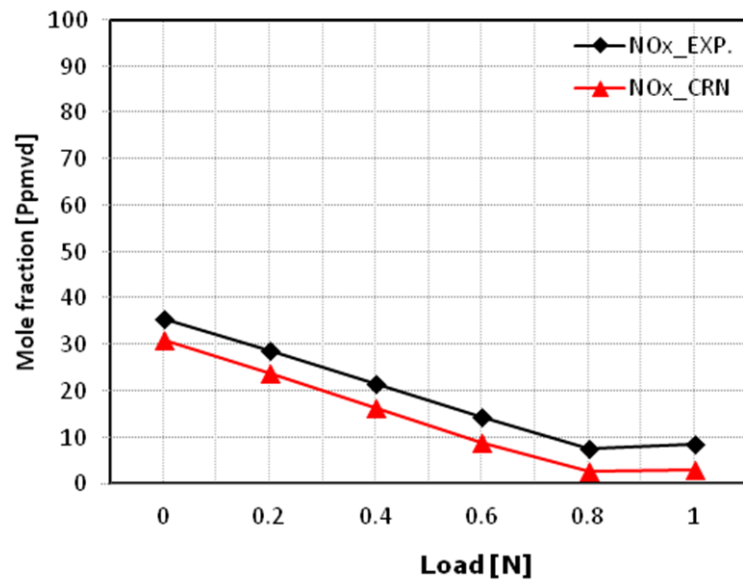
Figure 7. Non-uniformity mole fraction of NOx in normal condition
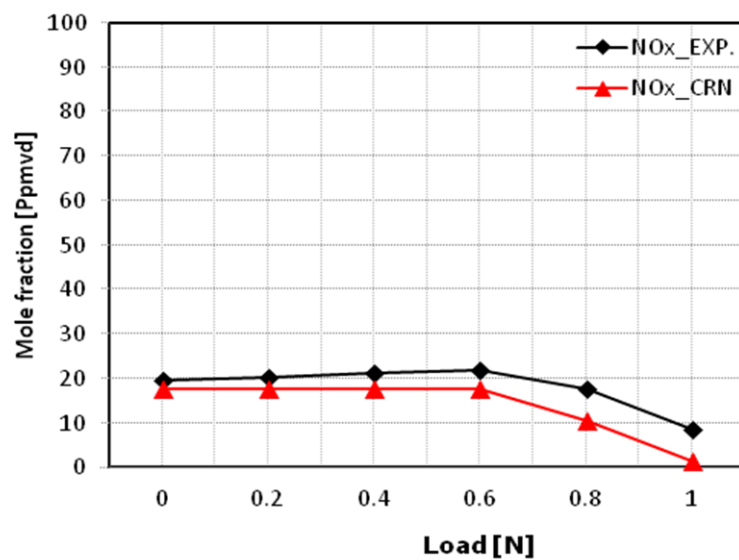
Figure 8. Non-uniformity mole fraction of NOx in cold condition
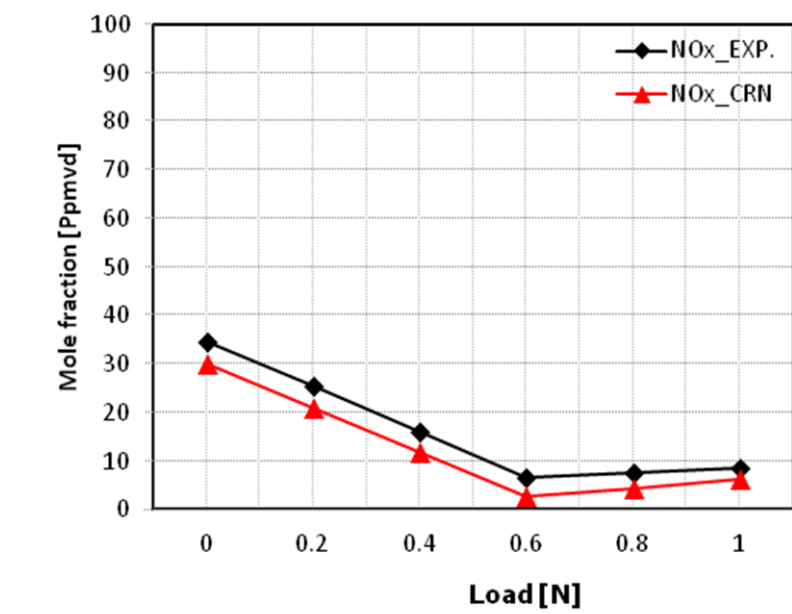
Figure 9. Non-uniformity mole fraction of NOx in hot condition
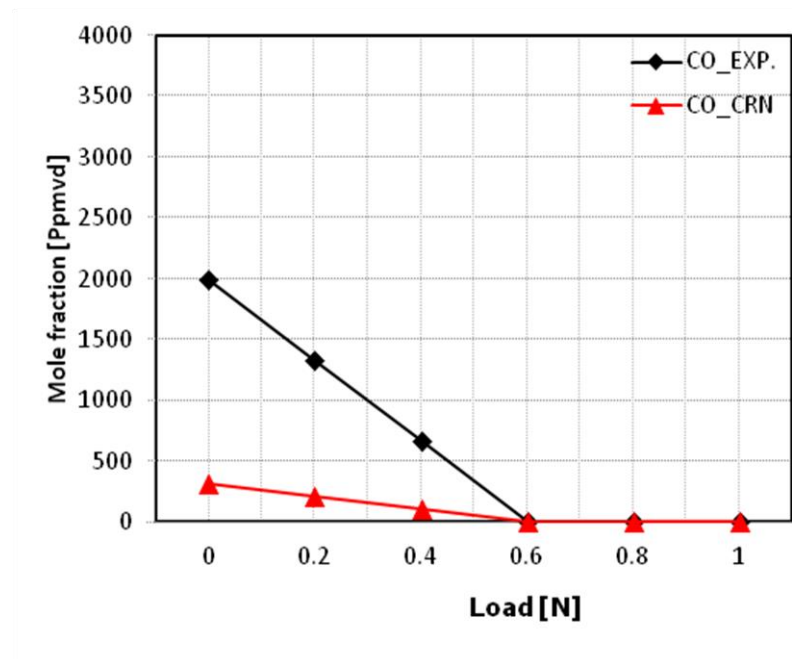
Figure 10. Non-uniformity mole fraction of CO in normal condition
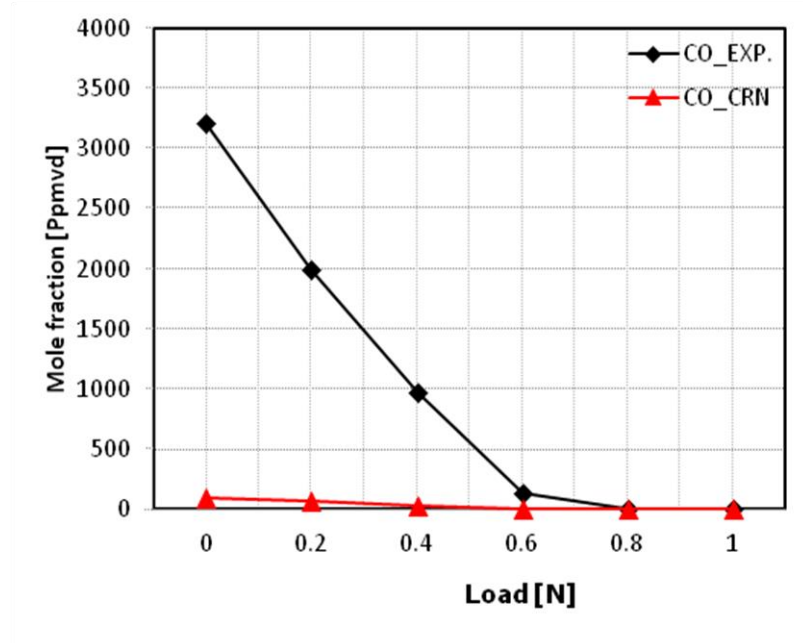
Figure 11. Non-uniformity mole fraction of CO in cold condition
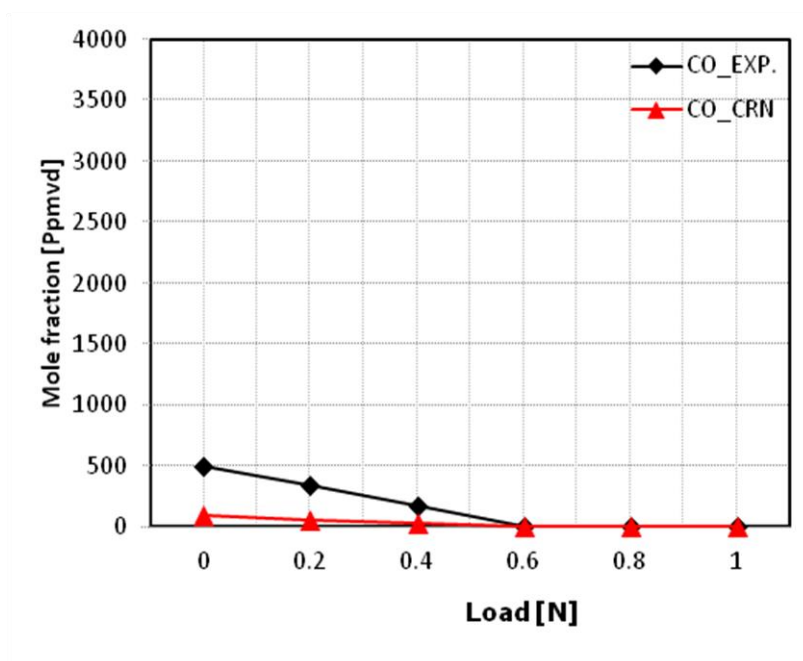
Figure 12. Non-uniformity mole fraction of CO in hot condition

The mole fraction of NOx in the normal condition is shown in Figure 7. The figure also shows the differences of each mole fraction of the NOx formation mechanism. The largest mole fraction of the NOx formation is at the idle load. The mole fraction of the NOx formation at the 0.6N load is lower than the idle load. Finally, the mole fraction of the NOx formation at the 0.8N load and the 1.0N load is equal to zero. At the 0.8N load and the 1.0N load cases, the temperature in the flame is high enough to trigger the thermal NOx production (Figure 4), so the mole fraction of NOx is low. However, the mole fraction of NOx that is exposed to this temperature is relatively small. Thus, the lowest mole fraction of the NOx formation is at the 0.8N load.

The mole fraction of NOx in the cold condition is shown in Figure 8. The figure also shows the contributions of each mole fraction of the NOx formation mechanism. The largest mole fraction of the NOx formation is at the 0.6N load. The mole fraction of the NOx formation at the 0.8N load is lower than the 0.6N load. Finally, the lowest mole fraction of the NOx formation is at the 1.0N load. The differences of the mole fraction of NOx compared to the normal condition show better results.

The mole fraction of NOx in the hot condition is shown in Figure 9. The largest mole fraction of the NOx formation is at the idle load. The mole fraction of the NOx formation at the 0.6N load and the 0.8N load is lower than the idle load. The differences of mole fraction of NOx in the 0.6N load and the 0.8N load between the experiment and the CRN simulation are zero.

Although the pilot flame has high temperature and species concentration as shown in Figure 7-9, a lot of NOx can be seen. The formation of NOx in the gas turbine combustor non-uniform inlet was applied using new modified CRN to predict the NOx emission, which is closer to the experimental data than the uniform inlet combustor, especially near the idle load.

Figures 10 ÷ 12 are used to show the mole fraction of the CO results in three CRN model conditions. The amount of CO at the low load appears significantly higher than others. Especially the mole fraction of CO in the cold condition is highest. The effect of the temperature on the formation of CO into the turbine combustor plays the role of the great importance.

The CO emission at the exit of the turbine combustor is essentially depended on the overall fuel-air equivalent ratio of the idle load, the 0.6N load, the 0.8N load, and the 1.0N load. The formation of CO in the gas turbine combustor non-uniform inlet was applied using new modified CRN to predict the CO emission, which is closer to the experimental data, especially near the 1.0N load.

Conclusions

The new CRN mechanism has been applied the CFD modeling of the gas turbine combustor in order to obtain the insight on the flow, the temperature, and the species fields. The flow field information from the gas turbine combustor CFD has been analyzed to determine the combustion zones in the combustor. These zones are modeled as the chemical reactor elements in CRN. The methodology of CRN development is determined based on the agreement between CFD and CRN models.

The new CRN model using the 24-idealized reactor scheme modeling has been developed based on the CFD results for the gas turbine combustor with the overall fuel-air equivalent ratio of the idle load, the 0.6N load, the 0.8N load, and the 1.0N load. The formation of the NOx and CO emissions in the turbine combustor non-uniform inlet prediction is closer to the experimental data, especially at the low overall equivalent ratio. This research has shown that:

- The combined CFD and CRN approach shows the ability to accurately predict the NOx and CO emissions for the lean premixed gas turbine combustor.
- The new CRN model by applying the non-uniform inlet is able to predict the NOx and CO emissions more accurate than the uniform inlet.
- The new CRN model can also be applied to the industrial combustors. The resulting CRN incorporates the important flow features and the boundary conditions such as: the fuel-air distribution, the velocity profile, the entrainment of the main recirculation zone and the main flame.

Nomenclature

CRN   : Chemical Reactor Network
CFD   : Computational Fluid Dynamic
CFM   : Coherent Flame Model
EBU   : Eddy Break Up
PPDF : Presumed Probability Density Function
CH_4 : Methane
CO   : Carbon monoxide
NOx : Nitrogen oxides
K   : Kelvin temperature scale
g_i : Gravitational acceleration component in direction x_i
k   : Turbulent kinetic energy
P   : Production term generation by normal stresses
P_B : Production term generation by buoyancy forces
P_{NL} : Production term generation by nonlinear models
S_{ij} : The mean strain
u_i : Absolute fluid velocity component in direction x_i
u_i' : Fluctuation fluid velocity component in direction x_i
ε   : Dissipation rate of the turbulent energy
μ   : Gas viscosity
$μ_t$: Turbulent viscosity
ρ   : Gas density
$σ_{h,t}$: Turbulent Prandtl number

References

[1] D.G. Nicol, P.C. Malte, and R.C. Steele, "Simplified models for NOx production rates in lean-premixed combustion," *ASME Paper 94-GT-432*, 1994.

[2] D.G. Nicol, R.C. Steele, N.M. Marinov, and P.C. Malte, "The importance of the nitrous oxide pathway to NOx in lean-premixed combustion," *Journal of Engineering for Gas Turbines and Power*, Vol. 117, pp. 100-111, 1995.

[3] K.U.M. Bengtson, P. Benz, R. Schaeren, and C.E. Frouzakis, "NyOx formation in lean premixed combustion of methane in a high-pressure jet-stirred reactor," In: *Proceedings of the Combustion Institute*, Vol. 27, pp. 1393-1401, 1998.

[4] R.C. Steele, *NOx and N2O Formation in Lean-Premixed Jet-Stirred Reactors Operated from 1 to 7atm*, Thesis (PhD), University of Washington, 1995.

[5] R.C. Steele, A.C. Tarrett, P.C. Malte, J.H. Tonouchi, and D.G. Nicol, "Variables affecting NOx formation in lean-premixed combustion," *Transactions of the ASME, Journal of Engineering for Gas Turbine and Power*, Vol. 119, pp. 102-107, 1997.

[6] T. Rutar, and P.C. Malte, "NOx formation in high-pressure jet-stirred reactors with significance to lean-premixed combustion turbines," *ASME Journal of Engineering for Gas Turbines and Power*, Vol. 124, pp. 776-783, 2002.

[7] D.G. Nicol, P.C. Malte, A.J. Hamer, R.J. Roby, and R.C. Steele, "Development of a five-step global methane oxidation-NO formation mechanism for lean-premixed gas turbine combustion," *ASME Journal of Engineering for Gas Turbines and Power*, Vol. 121, pp. 272-280, 1999.

[8] I.V. Novosselov, "Development and application of an eight-step global mechanism for CFD and CRN simulations of lean-premixed combustors," *ASME Journal of Engineering for Gas Turbines and Power*, Vol. 130, 2008.